

ENHANCED RAMAN EFFECT FROM CYANIDE ADSORBED ON A SILVER ELECTRODE

J. BILLMANN, G. KOVACS * and A. OTTO

Physikalisches Institut III, Universität Düsseldorf, D-4000 Düsseldorf, Fed. Rep. Germany

Received 28 June 1979; accepted for publication 29 August 1979

By the investigation of the cyanide silver system we show that the crucial condition for a 10^6 times enhanced Raman cross section is the roughness of the electrode surface on an atomic scale, e.g. by silver adatoms. The momentum conservation rule in electron–photon, electron–electron and electron–adsorbate interaction is broken by the presence of the atomic roughness. This leads to strong resonant Raman scattering from metal electrons and adsorbate vibrations.

1. Introduction

After the first detection of a Raman signal from an adsorbate on a silver metal electrode [1], it is now well established that in some cases there is a giant enhancement (about 10^6) of the Raman cross section of adsorbates at an electrode–electrolyte interface (e.g. pyridine on silver [2–4]), on metal colloids (pyridine on gold and silver [5]), at a metal–air surface (e.g. CN^- on silver [6]) and at a metal–vacuum surface (CO on silver [7]).

Numerous models for the enhancement have been proposed: The influence of the strong electric field at the electrode–electrolyte interface [8], the influence of image dipoles [9], a resonant Raman effect by coupling to surface plasmons involving roughness [10–12], resonant Raman effect due to different single particle excitation mechanisms [13–16], an analogy to electroreflectance [6,17,18], interference with roughness induced electronic Raman scattering [17,19], enhancement by dynamical charge transfer [13,20].

In all previous work on Raman scattering from silver electrodes [1–4,15, 23–25], the enhanced Raman signal was only found when the silver surface was reformed by one or several anodic oxidation–reduction cycles (see section 3).

Fleischmann and Hendra [1] subjected the silver electrode to cyclic linear potential sweeping for about 15 min between +200 and –300 mV in 0.1 M KCl, 0.05 M pyridine. Thus the effective surface area was increased by forming an extremely rough black surface [11,26]. Jeanmaire and Van Duyne [2] demon-

* NRC Canada postdoctoral fellow.

strated that after one single anodic cycle, with charge transfer of 25 mC cm^{-2} (corresponding to a dissolution and subsequent precipitation of a silver surface layer of about 250 \AA thickness), the Raman cross section for adsorbed pyridine was enhanced by about a factor of 10^6 .

Pettinger and co-workers [4,25] found that the Raman intensity from pyridine adsorbed on silver single crystal faces of orientation (111) and (100) was dependent upon the quantity of reformed solid silver, given in monolayers of silver. Between 0.03 and 9 monolayers, the Raman signal was growing exponentially. Within the sensitivity of electroreflectance and high energy electron diffraction (RHEED), no roughening of the silver surface was observed.

Therefore, an explanation based on an increase of surface area can safely be excluded.

So, what is the significance of the anodic cycle? One might think of three possibilities:

- (a) An electrochemical reaction is forming a surface complex, which would not exist without the anodic cycle.
- (b) By the anodic cycle, a co-adsorbate is formed (e.g. adsorbed oxygen), enhancing the Raman cross section in some unknown way.
- (c) The structure of the silver surface (on an atomic scale) is changed by the anodic sweep.

To study the enhancement and the significance of the anodic cycle, we have chosen the system cyanide on a silver electrode, following some previous work [6, 15, 17,21,22], by Furtak and one of the authors. Because $(\text{CN})^-$ is isoelectronic to CO, one may hope to profit from the vast literature of CO chemisorption for the interpretation of $(\text{CN})^-$ chemisorption and also to apply the same computational methods.

It is the aim of the work reported here to understand why the anodic oxidation–reduction cycle of the silver electrode is necessary to gain enhanced Raman scattering and to assign the observed vibrations of $(\text{CN})^-$ chemisorbed on silver. The sections 2–7 give a comprehensive account of our experimental work. In sections 8 and 9, we propose in a short version a microscopic model of the enhancement effect.

2. Experimental set up

The sample, the working electrode W in fig. 1, was a polycrystalline silver slug of 9 mm diameter, whose lower surface was immersed in the electrolyte. Before every new electrochemical Raman experiment, the sample was etched in a mixture of H_2O_2 and NH_4OH . In some cases we also used evaporated silver films, which yielded the same results as the silver slug. The electrolyte was 0.1 M Na_2SO_4 or 0.1 M Na_2SO_4 with 0.01 M KCN; it was purged by oxygen-free nitrogen. The reference electrode was a saturated calomel electrode (SCE) separated from the electrochemical main cell by a bridge tube with vycor tip. The counter electrode was a platinum

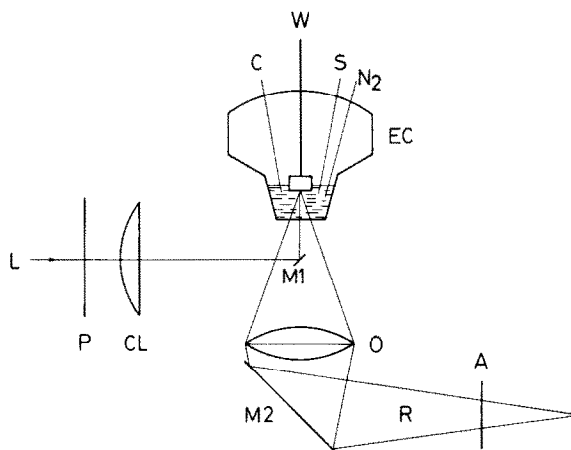


Fig. 1. Raman backscattering from the silver electrolyte interface. L laserbeam, A analyzer, CL cylindrical lens, M1, M2 mirrors, O 1 : 1 aperture objective, R Raman scattered light cone, P polarizer, EC electrochemical cell, C counterelectrode, W working electrode, S saturated calomel electrode, N₂ nitrogen inlet.

wire. The voltage between sample and reference electrode was controlled by a potentiostat–galvanostat with integrated coulombmeter. In general, laser light from an Ar⁺ laser was incident perpendicular to the silver surface, its polarization could be chosen by rotating a Fresnel prism. Focussing onto the silver surface was achieved by a cylindrical lens ($f = 150$ mm). The incident power at the sample was of the order of 200–500 mW. The scattered light was analyzed with the help of a double monochromator with holographic gratings, wavelength drive and standard photon counting equipment. Because of normal incidence of the laser light, depolarization ratios could be measured by rotating the polarization of the incident light, keeping the polarizer P in fig. 1 in fixed position.

3. Electrochemical measurements

Different voltammograms for the 0.1 M Na₂SO₄ aqueous electrolyte and the 0.1 M Na₂SO₄ 0.01 M KCN electrolyte are depicted in fig. 2. Whereas the pH value for the 0.1 M Na₂SO₄ electrolyte is about 5, the pH value is changed to about 11 in the mixed electrolyte of 0.1 M Na₂SO₄ and 0.01 M KCN. This may be calculated from the dissociation constant of HCN and is corroborated by measurements with pH paper. The low H⁺ concentration is caused by formation of undissociated HCN. Nevertheless, about 99% of the cyanide from the 0.01 M KCN are still free CN⁻ ions. According to the Pourbaix diagrams of the Ag–H₂O [27] and CN–H₂O

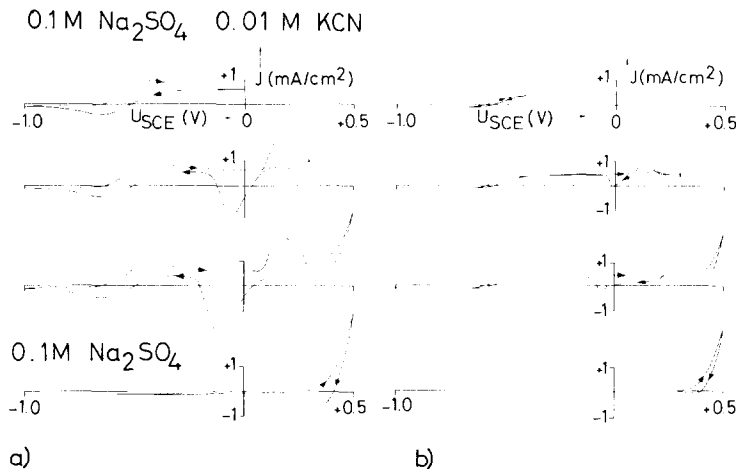


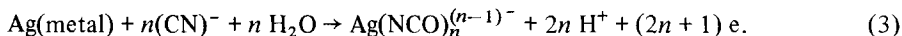
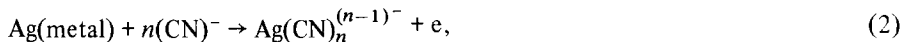
Fig. 2. Voltammogram from -1.0 to $0, 0.3, 0.5$ V and immediately back to -1.0 V at 50 mV/s (a), 5 mV/s (b) in 0.1 M Na_2SO_4 , 0.01 M KCN aqueous solution and one sweep from -1.0 to $+0.5$ V and immediately back at 50 mV/s (a), 5 mV/s (b) in 0.1 M Na_2SO_4 aqueous solution.

system [28] (see fig. 3), the positive current (corresponding to electron transfer into the silver electrode) above about 0.3 V for the pure Na_2SO_4 electrolyte is caused by the oxidation of silver which goes into solution as a free ion:



Only part of the dissolved quantity of Ag^+ is reduced in the form of metallic silver on the electrode surface – the rest has been lost by diffusion into the electrolyte. This is indicated by the relatively low negative current in the cathodic sweep (decreasing voltage versus SCE) compared to the anodic sweep (increasing voltage versus SCE).

The increase in anodic current at about -0.6 V in the 0.1 M Na_2SO_4 0.01 M KCN electrolyte corresponds to the dissolution of silver as silver cyanide or silver isocyanate complexes:



At about -0.3 V, a constant current density of about $400 \mu\text{A}/\text{cm}^2$ is reached due to process (2) or (3). The observed hysteresis in this range is caused by different concentrations of silver cyanide complex ions in front of the electrode in the anodic and cathodic sweep. If the cathodic sweep is performed with $dU/dt = -50$ mV/s, some of these complexes are reduced to Ag , $(\text{CN})^-$ (and H_2O). At $dU/dt = -5$ mV/s, this is no more the case.

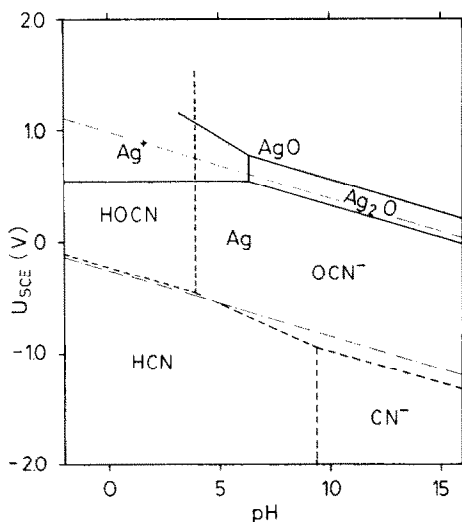
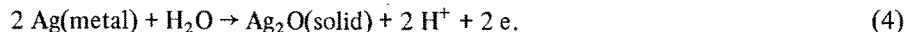


Fig. 3. Pourbaix diagrams of the systems Ag–H₂O (—) and (CN)[−]–H₂O (---). The potentials correspond to 1 : 1 concentration of the partners of the respective redox system. Dashdotted lines correspond to the thermal equilibrium dissociation of water, upper line oxygen evolution, lower line hydrogen evolution.

The strong increase in the anodic current at about 0.1 to 0.3 V corresponds to the formation of an Ag₂O surface film by



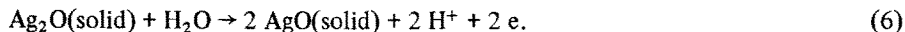
According to the Pourbaix diagram in fig. 3, at a pH value of 11, one has to expect the formation of solid Ag₂O in this voltage range. The reversed reaction (4) causes the current minima in the cathodic sweeps around −0.1 V. Ag₂O is not soluble in water. Nevertheless, silvercyanide complexes go into solution also in the presence of the Ag₂O film as indicated by the current of about 400 μA/cm², on which the current maxima and minima due to reaction (4) are superimposed.

Probably the Ag₂O film is dissolved at the Ag₂O–electrolyte interface by



and is growing at the Ag₂O–Ag interface by reaction (4). For the following, it is important to note that metallic silver is reformed at the electrode surface when the Ag₂O film is reduced at about −0.1 V.

As in the pure Na₂SO₄ electrolyte, one observes the onset of a further electrochemical reaction at 0.3 to 0.5 V. According to the Pourbaix diagram (fig. 3) this corresponds to



The reversed reaction (6) is responsible for the structure around +0.2 V in the cathodic sweep.

After completing the cycle to -1.0 V there is no electrochemical indication for surface films beyond monolayer thickness.

4. Raman measurements

After insertion of the silver sample into the electrolyte at about -1.0 V and before any voltage sweep, there was only a background signal from the electrolyte (fig. 4). The slope from 250 – 900 cm^{-1} and the weak peaks near 1618 and 2100 cm^{-1} are due to liquid water [29], the line at 982 cm^{-1} is a vibration of the SO_4^{2-} ion.

However, a very strong Raman signal is obtained after stepping for 5 s to $+0.5$ V and stepping back to voltages between -0.7 to -1.0 V. This spectrum is identical to the spectrum published by Furtak [15]. As discussed in section 6, this signal is probably due to an $\text{Ag}(\text{CN})_3^-$ surface complex. Raman spectra from the electrode surface were taken at different points of the voltammogram in fig. 2 – that means, the sweep was stopped at several voltages within the anodic or cathodic sweep and a Raman spectrum was recorded. In the voltage range from about -0.7 to -1.0 V, the strong Raman signal was only existent after the anodic stepping described above or after the pre-treatments described in section 5. No surface specific signal was

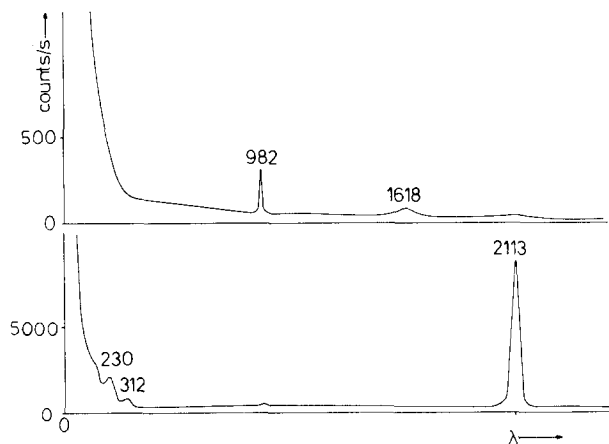


Fig. 4. Raman spectra from a polycrystalline silver electrode at -1.0 V in 0.1 M Na_2SO_4 , 0.01 M KCN aqueous electrolyte, before any anodic sweep (above) and after switching for 5 s to $+0.5$ V (below). Spectra have been taken in backscattering configuration without polarizer (fig. 1), with laser wavelength 5145 Å, abscissa is linear in wavelength, stokes shifts of maxima are given in cm^{-1} .

found in the range of dissolution of metallic silver as silver cyanide complexes (about -0.7 to 0.1 V). When an Ag_2O layer was on top of the metallic silver (between 0.2 to 0.3 V), we observed sometimes two lines at 273 and 2165 cm^{-1} on a higher background than that from the electrolyte. These frequencies are characteristic of bulk AgCN [6] (see section 6).

The Pourbaix diagram in fig. 3 may lead to the expectation of a Raman signal of silver isocyanate AgNCO . To check this possibility, we have precipitated AgNCO from mixing an AgNO_3 aqueous solution with KNCO solution. The Raman spectrum in fig. 5 shows the asymmetric stretch vibration of the linear NCO group at 1328 cm^{-1} , the symmetric vibration at 2270 cm^{-1} . (For the assignment see ref. [30].) There is no resemblance with the spectrum in fig. 4. However, when silver is electropolished in cyanide solution and exposed to air under rather poorly defined conditions, one observes a line at 1324 cm^{-1} [17] which is probably due to AgNCO (see fig. 5).

In contrast to the cyanide ion, the NCO^- bonds to silver via the nitrogen atom [31]. Thus the oxidation of CN^- to NCO^- in the adsorbed state would involve a flip over of the CN group.

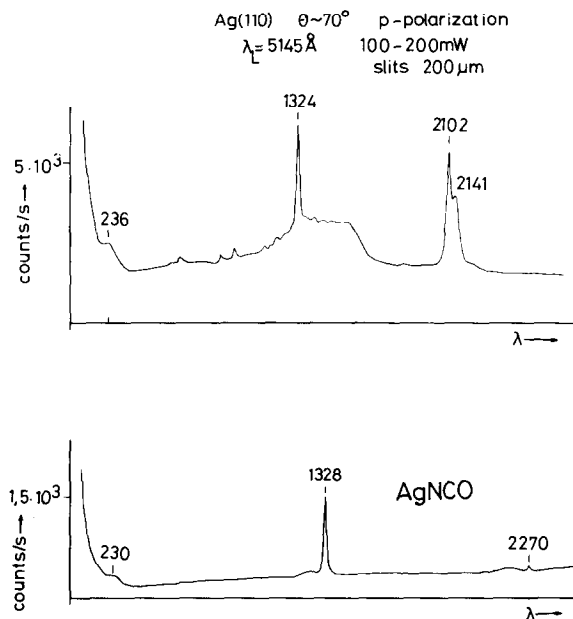


Fig. 5. Upper spectrum: Raman spectrum of a $\text{Ag}(110)$ surface, electropolished in air saturated solution of 5 g KCN , 9.5 g KCO_3 , 13 g $\text{KAg}(\text{CN})_2$ in 250 ml H_2O at about 0.1 A/cm^2 for 5 min, rinsed in distilled water, exposed to air. Lower spectrum: Raman spectrum of freshly precipitated AgNCO , in aqueous medium.

5. The formation of a new silver surface by reduction of silver

To decide between the three possibilities to explain the necessity of the anodic sweep (see section 1), the following experiments were performed:

Starting with the silver sample in pure 0.1 M Na_2SO_4 electrolyte at -1.0 V, stepping for 5 to $+0.5$ V, KCN solution was added only afterwards at -1.0 V to yield 0.01 M KCN concentration. After adding the cyanide, the Raman spectrum was similar to the result for cyanide present during the anodic cycle (fig. 4). This excludes the first possibility, namely the exclusive formation of the silver cyanide surface complex by anodization. However, a new silver surface has been formed by reduction of Ag^+ (process (1)) as discussed in section 3.

The following experiment excludes a possible influence of coadsorbed oxygen: The anodic cycle was performed in 0.1 M H_2SO_4 . Up to $+0.5$ V, at the pH value 0 to 1, there is no chance for oxygen evolution at the silver surface (see fig. 3). After completing the anodic cycle, the electrolyte was neutralized by 0.2 M NaOH at -0.3 V, and 0.01 M KCN added at -1.0 V. There was again a strong Raman signal like in fig. 4. In this experiment also, a new silver surface was formed.

Apparently, the necessary precondition for an enhanced Raman signal is the formation of a new silver surface: As discussed in section 3, in the 0.1 M Na_2SO_4 0.01 M KCN electrolyte, metallic silver is reduced on the electrode surface only when solid Ag_2O has been formed before. Therefore, a new silver surface is formed only by those anodic sweeps which have their maximum voltage above 0.2 V. Indeed, only for those sweeps does one observe the strong Raman signal around -1.0 V, provided that the cathodic sweep velocity is not much slower than 50 mV/s. When the cathodic sweep is performed too slowly, the new silver surface formed by reduction of Ag_2O is dissolved by the formation of silver cyanide complexes which go into solution (reactions (2) and (3)). For instance, when the electrochemical cycle is stopped at about -0.2 V after the reduction of Ag_2O and an additional charge of about 0.02 As cm^{-2} is transferred by dissolution of metallic silver as cyanide complexes, and subsequently the cathodic sweep to -1.0 V is completed with 2 mV/s, the signal at 2113 cm^{-1} is lost completely.

What would be different on a newly formed silver surface with respect to the original surface? The original one is either formed by etching a polycrystalline silver slug or by evaporating a silver film. In both cases one might expect, in small scales, thermodynamically stable surfaces with only a small number of silver adatoms sitting on the surface lattice planes or on surface terraces: For etched samples, these adatoms would most likely go into solution. For evaporated samples, surface atoms have a relatively high surface mobility and growth rates are only of the order of 1–10 monolayers per second. Hence, surface atoms will most probably be captured at steps and kinks and the resulting films will be smooth on atomic scale.

On the other hand, when hydrated Ag^+ ions are discharged at a silver electrode, this process is diffusion controlled. Surface diffusion is more difficult due to the presence of an adsorbed water layer.

This explains, first, that the growth rate determining step in electrocrystallization of silver single crystals is the linear growth of surface layers of monoatomic step height [33], and second, that the incorporation of Ag atoms at the kinks of these steps is directly from the electrolyte and not by surface diffusion of adatoms [34].

In the electrocrystallization experiment [33,34], current densities are in the range of 10^{-5} A cm⁻² and overpotentials in the range of some mV. Additionally there is a high concentration of Ag⁺ in solution, so that the direct incorporation of silver atoms at kinks sites is not limited by lack of Ag⁺ ions near the kink site.

On the other hand in the anodic stepping procedures described here, current densities are some orders of magnitude higher, overpotentials in the range of 100 mV.

As the amount of reducible Ag⁺ is limited, the concentration of Ag⁺ is going to zero during the reduction. Therefore, one has to expect as result of the fast reduction a high density of small nucleation centers because of low lateral growth rate and finally a non negligible surface concentration of adatoms. In this respect, it is interesting that silver has the lowest surface energy with respect to all transition and noble metals [35], and therefore the greatest stability of adatoms.

Anyway, the transformation of an originally smooth silver surface to the extremely rough surface by repeated anodic cycling [11,26] or by the dendritic growth of silver by cathodic reduction of Ag⁺ [36] must have some intermediate state where roughness exists on an atomic scale. In the early stages, this atomic roughness may well escape the detection by methods like RHEED and optical reflection spectroscopy.

The necessary precondition of the formation of a new silver surface with atomic scale roughness is confirmed by a cathodic sweep to negative voltages up to -3.0 V in the presence of Ag⁺ ions or Ag(CN)₂⁻ complexes in the electrolyte. In this case, no bulk silver is dissolved like in the anodic sweep to 0.5 V but Ag⁺ or the silver cyanide complexes are reduced to metallic silver at the silver electrode [32].

Between -1.0 and -2.0 V, in 0.1 M KAg(CN)₂ solution and in 0.01 M AgNO₃ solution, starting with a smooth electrode, about 25 monolayers of silver are reduced per second. In this case no Raman signal from a surface adsorbate can be obtained, when stepping to -1.0 V (and adding KCN to the solution in the case of the silvernitrate electrolyte). One has to conclude, that the silver electrode remains smooth.

However, if silver is reduced in the presence of the strong hydrogen evolution between -2.0 and -3.0 V, one obtains the strong Raman signal at -1.0 V. Apparently, hydrogen evolution interferes with the reduction of silver, thus leading to a rough electrode surface (the details of this process are still under investigation). On the other hand, when the silver electrode was made cathodic at -3.0 V in KCN solution, and KAg(CN)₂ was added at -1.0 V, the result was negative. In this case, no silver was reduced at the silver electrode.

The results of these experiments make it very unlikely that the enhancement is

due to a coadsorbate, because for anodic and cathodic sweeps the coadsorbate should be different, the enhancement effect is the same, however. The SO_4^- ions are without any importance as was proved in less detailed experiments in 0.1 M KCl, 0.01 M KCN and 0.1 M and 0.01 M KCN electrolytes, where spectra like in fig. 4 could be obtained by suitable anodic oxidation–reduction cycles.

One should note that in this section we have discussed roughness on a much finer scale than the comparatively macroscopic roughness which couples photons with surface plasmons in the various theoretical proposals for the enhancement effect involving surface plasmons and roughness [10–12].

The hypothesis of the significance of isolated Ag atoms on the silver surface is supported by the steric arrangement of the $\text{Ag}(\text{CN})_3^-$ surface complex as described in the next section, and by considerations concerning the enhancement mechanism (see sections 8 and 9).

6. Silver cyanide surface complexes

It is well known that the following silver cyanide complex ions may exist in aqueous solution: $\text{Ag}(\text{CN})_2^-$, $\text{Ag}(\text{CN})_3^-$, $\text{Ag}(\text{CN})_4^-$ [37–39]. In solid form, only AgCN [49] and salts like $\text{KAg}(\text{CN})_2$ [41] and $\text{K}_3\text{Ag}(\text{CN})_4$ exist [37]. The bonding of the $(\text{CN})^-$ group to silver in the complexes is via the C atoms [40] (this follows also from structural evidence of Cu and Au cyanide complexes). Without exception, it is assumed in the literature that the $\text{Ag}(\text{CN})_2^-$ ion in solution is linear, similar to its structure in $\text{KAg}(\text{CN})_2$ [41]. It is also assumed that $\text{Ag}(\text{CN})_4^-$ is tetrahedral like the $\text{Cu}(\text{CN})_4^-$ tetrahedron in solid $\text{K}_3\text{Cu}(\text{CN})_4$ [43]. The $\text{Ag}(\text{CN})_3^-$ may have pyramidal symmetry C_{3v} or planar symmetry D_{3h} . Jones and Penneman [38] proposed a tetrahedral coordination of the $(\text{CN})^-$ groups and one water molecule around the silver atoms.

The relevant observed CN-stretch vibrations are compiled in table 1. The overall trend

$$\omega_{\text{CN}} < \omega_{\text{Ag}(\text{CN})_4} < \omega_{\text{Ag}(\text{CN})_3} < \omega_{\text{Ag}(\text{CN})_2} < \omega_{\text{AgCN}},$$

may be explained by increasing bonding to silver via the 5σ orbital of the $(\text{CN})^-$ ion [47,48]. The 5σ orbital of CO and $(\text{CN})^-$ is a bonding orbital between the metal and the ligand, but antibonding with respect to intra ligand bonding. Therefore, increasing 5σ metal ligand bonding should increase the ligand stretch vibration frequency. This effect is compensated in carbonyles by electron backdonation into the antibonding 2π orbital of CO [47]. For cyanides, however, the antibonding nature of the 5σ orbital is much stronger than that for CO as derived from the calculation of so-called 5σ overlap populations for CO and $(\text{CN})^-$ [48]. Therefore, the increase in the CN stretch vibration due to 5σ bonding is not fully compensated by backdonation to 2π [48], and there is a net increase of the $(\text{CN})^-$ stretching frequency with increasing Ag–CN bonding. In solid AgCN, there are Ag–CN–Ag–

Table 1
 Frequencies and assignment of CN stretching vibrations: abbreviations: IR = infrared, R = Raman, ν_s = totally symmetric mode, ν_a = non-totally symmetric mode, str = strong, m = medium

	IR		R	This work (R)
(CN) ⁻ _{aqueous}	2080	[38]		2080 ± 1
KCN _{solid}			2096	[6]
Ag(CN) ₄ ⁻ _{aqueous}	2092	[38]	2097 (ν_{symm} , ν_{anti}) 2094 (dep., ν_{anti}), 2098 (pol., ν_{symm})	[46] [45]
K ₃ Ag(CN) ₄ _{solid}	2097 str	[38]		
	2091 m	[38]		
Ag(CN) ₃ ⁻ _{aqueous}	2105	[38]	2108 (g ν_{symm} , ν_{anti}) 2107 (dep., ν_{anti}), 2110 (pol., symm)	[46] [45]
Ag(CN) ₂ ⁻ _{aqueous}	2135 (ν_{anti})	[38]	2141 (ν_{symm}), 2139 (ν_{symm})	[44], [46]
K Ag(CN) ₂ _{solid}	2139 (ν_{anti})	[38]	2146 (ν_{symm})	[40]
	2140 (ν_{anti})	[40]		
AgCN _{solid}	2164	[38]	2165	[6]
				2111 ± 1 (ν_{symm}) 2109 ± 1 (ν_{anti}) 2143 ± 1

CN chains [49], and perhaps there is also some Ag–N bonding like in the isocyanates. If this involves also the $(\text{CN})^-$ 5σ orbital (according to ref. [50], the 5σ orbital of $(\text{CN})^-$ has about equal weight on the carbon and the nitrogen side), the additional 5σ bonding in AgCN would contribute to its high CN stretch vibration frequency.

For the CN stretch vibration of the $\text{Ag}(\text{CN})_3^-$ complex, point group analysis yields for $\text{C}_{3v}(\text{D}_{3h})$ symmetry one totally symmetric $\text{A}_1(\text{A}'_1)$ and a double degenerate $\text{E}(\text{E}')$ mode, both modes Raman active, the degenerate mode also infrared active. The difference in frequency between these modes is not more than 3–5 cm^{-1} (see table 1) as confirmed by our own results from depolarization measurements.

In fig. 6, we compare the spectrum of the silver-cyanide complex ions in a solution of 0.5 M KCN, and 0.18 M $\text{KAg}(\text{CN})_2$ with the spectrum from the polycrystalline Ag electrode after the treatment described in section 5 at -1.0 V versus SCE.

At the relatively low concentration of cyanide and silver in that solution, the signal from $\text{Ag}(\text{CN})_4^{2-}$ complex is missing. At higher overall concentrations, this signal appears at around 2095 cm^{-1} as already observed by Chantry and Plane [46]. This is in agreement with the equilibrium constants of the silver cyanide complexes of Jones and Penneman [38].

The CN^- coverage of the electrode after one cycle from -1.0 C to $+0.3$ V and back to -1.0 V is $(0.6 \pm 0.12) \times 10^{15} \text{ cm}^{-2}$ as measured with $(\text{C}_{14}\text{N})^-$ as radioactive tracer in the 0.1 M Na_2SO_4 , 0.01 M KCN electrolyte by Pütz and Heitbaum [51]. This is corroborated by the results of Bergman et al. [52] who find a coverage between 0.8 and $1.4 \times 10^{15} \text{ cm}^{-2}$ after stepping from -0.95 to $+0.5$ V and back for 0.1 to 20 s. (See also the older work of ref. [53].) A smooth silver (111) surface has 1.38×10^{15} silver atoms/ cm^2 for comparison.

The increase of the Raman cross section for the adsorbed CN with respect to free $(\text{CN})^-$ in solution was measured to be 10^6 – 10^7 . This is of the same order as for pyridine adsorbed on silver [2]. As pointed out in sections 7 and 9 we believe that the Raman cross section is considerably increased only for those CN^- ions, bound to an atomic scale surface roughness. Hence, the enhancement could even be greater.

The coincidence of the CN stretch frequency of the adsorbate and of free $\text{Ag}(\text{CN})_3^-$ indicates that the surface adsorbate is probably a pyramidal $\text{Ag}(\text{CN})_3^-$ complex on top of densely packed terraces which are atomically plane over some lattice constants (see fig. 7). Once there are silver adatoms on such terraces (whose possible creation has been described in section 5) such a pyramidal complex may easily be formed without distortion from its postulated C_{3v} geometry in solution [38]. When three CN^- ions are attached to such a silver adatom and form the $\text{Ag}(\text{CN})_3^-$ surface complex, the Ag adatom will partly be ionized to $\text{Ag}^{+\epsilon}$. From steric considerations, the other possibilities would be an $\text{Ag}(\text{CN})_2^-$ surface complex which would be distorted from its linear form in solution and a simple linear Ag–CN complex perpendicular to the surface.

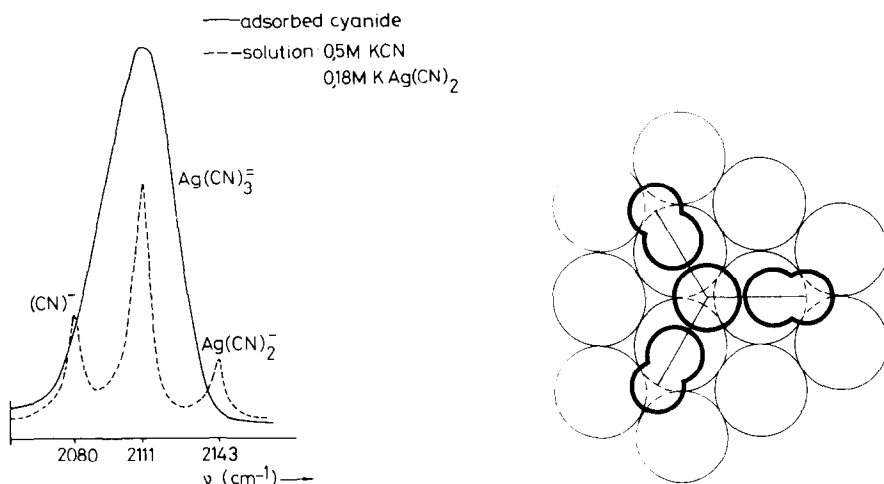


Fig. 6. Dotted line: Raman spectrum from a 0.5 M KCN, 0.18 M $\text{KAg}(\text{CN})_2$ aqueous solution, with assignment to CN stretch vibration of $(\text{CN})^-$, $\text{Ag}(\text{CN})_3^-$ and $\text{Ag}(\text{CN})_2^-$. Full line: Raman spectrum from the cyanide adsorbate on a polycrystalline silver electrode, after electrochemical treatment see in fig. 4.

Fig. 7. Model of a $\text{Ag}(\text{CN})_3^-$ surface complex on a silver (111) terrace. The $\text{Ag}^+ - \text{N}$ distance corresponds to the value for $\text{KAg}(\text{CN})_2$ [41,42], the CN distance to the value found in $\text{KAu}(\text{CN})_2$ [42]. The direction of the three CN axis with respect to the normal has been assumed like the angles between the connection lines between the middle and corner points of a regular tetrahedron. Radii correspond to Paulings covalent radii for Ag^+ (ca. 1.12 Å), C (ca. 0.85 Å) and N (ca. 0.75 Å).

We think that the CN stretch frequency of undistorted complexes is not much altered by adsorption because the changes in coordination involve only second nearest neighbors of the CN groups [54,55].

There are also indications for an enhanced Raman effect from other silver cyanide surface complexes: On a (110) single crystalline Ag surface, etched electrochemically in a cyanide solution and exposed to air, a Raman line was found at 2141 cm^{-1} apart from one at 2102 cm^{-1} (see fig. 5). This may be indicative of an $\text{Ag}(\text{CN})_2^-$ surface complex [17] (see table 1). One might speculate that the two $(\text{CN})^-$ groups are attached perpendicular to the direction $(\bar{1}10)$ of the edges and grooves of silver surface atoms. In the presence of an Ag_2O layer, there is a Raman signal corresponding to bulk AgCN (see section 4). It is possible that this signal is due to an AgCN complex linearly coordinated to the rough silver surface sitting underneath the Ag_2O layer.

The Ag–CN stretching and Ag–C–N bending frequencies have to be expected by analogy to data from $\text{Ag}(\text{CN})_2^-$ [40] and $\text{Cu}(\text{CN})_4^-$ [57] between 200 and

400 cm^{-1} . These vibrations probably account for the observed peaks at 230 and 312 cm^{-1} in fig. 4, though an analysis is not yet possible.

7. The significance of atomic scale surface roughness

We have shown that an enhanced Raman signal from adsorbed cyanide is only found after formation of a silver surface which is rough on an atomic scale.

In this work, roughness has been created by electrochemical means, but apart from this, the electrolytic environment of the surface adsorbate seems to be unimportant. Therefore, other ways to produce atomic roughness should also yield the same results for the given system.

This is corroborated by previous results of one of the authors [6]: when a silver surface is mechanically polished in air, one observes a strong Raman signal due to adsorbates out of the air.

One might argue that cyanide is only adsorbed on a rough surface and hence the enhanced Raman signals can only be observed from a roughened surface.

This is ruled out by the measurements of Pütz and Heibaum [51]: On a smooth silver electrode, exposed to the electrolyte for 5 min at -0.65 V, one finds a CN^- coverage of $(0.83 \pm 0.16) \times 10^{15} \text{ cm}^{-2}$, and after a cycle from -1.0 to 0 V back a coverage of $(0.78 \pm 0.15) \times 10^{15} \text{ cm}^{-2}$ comparable to the coverage after the anodic roughening cycles. (See section 6.)

Finally, one might argue that only a special silver cyanide surface complex shows the enhancement effect (e.g. $\text{Ag}(\text{CN})_3^{\ominus}$) and that this complex does not exist at smooth surfaces. We think that this is very unlikely because we have presented evidence for an enhanced Raman effect also for other adsorbed silver cyanide complexes (AgCN , $\text{Ag}(\text{CN})_2$), see section 6. Fig. 5 shows an enhancement also for silver surface complexes with NCO and the carbonate group [6]. Raman enhancement has been found for many molecules adsorbed to silver but only after the anodic cycle treatment [2,23].

Therefore, we conclude that roughness on an atomic scale is crucial for the occurrence of an enhanced Raman effect. We conjecture that, once a molecular group is bound to an adatom, a step or any other kind of atomic scale surface roughness, the Raman effect will be enhanced.

In the next section, we will give a short outline of a model which explains the enhanced Raman effect by the atomic scale surface roughness.

8. Roughness induced electronic Raman scattering

It was first pointed out by one of the authors [17] that a Raman signal from the vibrations of an adsorbate is always superimposed on a strong background. For instance in fig. 4, the general background in the enhanced spectrum is stronger than

the Raman signal from the electrolyte. It was first conjectured by this group [17] that this might be due to roughness induced electronic Raman scattering [17,19]. Like Burstein and co-workers [19], we observed that the background signal is completely depolarized.

We think that the background is mainly caused by third order electronic Raman scattering described by

$$\sigma(\omega_k) \sim \left| \sum_{i,j} \frac{\langle 0 | H_{ep} | j \rangle \langle k, j | H_{ee} | i \rangle \langle i | H_{ep} | 0 \rangle}{(\omega_L - \omega_k - \omega_j)(\omega_L - \omega_i)} + \text{time ordered terms} \right|^2. \quad (7)$$

In (7), $\sigma(\omega_k)$ is the Raman cross section for the Stokes shift ω_k , ω_L is the laser frequency, i, j and k denote electron hole pairs, H_{ep} corresponds to the $e(\mathbf{pA} + \mathbf{Ap})/2mc$ term of electron–photon interaction and H_{ee} is the electron–electron interaction. H_{ep} and H_{ee} are different from the corresponding quantities in the bulk metal or in the free electron gas since additional momentum is available for scattering of the electron hole pairs i and j at the adatoms or at other atomic scale surface roughness. This may be made plausible by the following arguments:

In the bulk of a nearly free electron metal scattering of electrons by the atomic cores is weak because momentum transfer is restricted to reciprocal lattice vectors and the form factors for these processes turn out to be small. This is not true for adatoms. In this case, the broken lattice symmetry allows any momentum transfer and the form factors will be much larger for a wide range of momentum transfer. Such scattering processes account also for the well known increase of the resistivity of thin metallic films if the surface is rough on an atomic scale [59].

Because of the relaxation of the momentum conservation rule, the electron hole pairs i, j, k , for which the matrix elements in (7) are non zero, do extend over the whole single particle excitation band, whereas with momentum conservation, only very small portions of the single particle excitation band would be involved in (7). With relaxation of the momentum conservation, matrix elements do exist also for those electron hole pairs, for which the denominators in (7) become zero. As explained by Martin and Falicov [60], a cross section like in formula [7] for a continuum of intermediate states i and j is resonant. For constant numerator it is proportional to the square of the product of the electronic susceptibilities at ω_L and $\omega_L - \omega_k$. In our case, these susceptibilities would correspond to the additional surface susceptibility by the formation of atomic scale roughness.

There exists also an analogy to the resonant Raman scattering from dyes, which also have a broad continuum of electronic excited states. In this case, the cross section could be considered as analogous to formula (7), where H_{ep} is replaced by the interaction of photons with the valence electrons of the dye molecule, and H_{ee} by the interaction of these valence electrons with the dye molecule vibrations, i and j would correspond to excited vibronic states, Hence we conclude by analogy, that the first term in (7) is resonant. As the directions of the vector potential \mathbf{A} of the incident light in $\langle i | H_{ep} | 0 \rangle$ and of the scattered light in $\langle 0 | H_{ep} | j \rangle$ are uncorrelated, the scattered radiation will be depolarized.

More experimental evidence for the existence of roughness induced electronic Raman scattering will be presented elsewhere [61].

9. Roughness induced enhancement of the Raman scattering from adsorbates

Like Chen and Burstein [19] we observed that the Raman line of the CN stretch mode (see fig. 4) is completely depolarized like the background. We think that this indicates a common origin of the enhancement of the Raman scattering cross section of the vibrations of the adsorbate and of the background signal (see also Chen and Burstein [19]). Our model is within the philosophy of local scattering processes of electron hole pairs as outlined by Burstein et al. [13,58]. However, starting from our experimental results, we put more emphasis on the local roughness. We propose that the cross section is given by formula (8)

$$\sigma(\omega_v) \sim \left| \sum_{i,j} \frac{\langle 0 | H_{ep} | j \rangle \langle 1, j | H_{ev} | 0, i \rangle \langle i | H_{ep} | 0 \rangle}{(\omega_L - \omega_v - \omega_j)(\omega_L - \omega_i)} + \text{time ordered terms} \right|^2, \quad (8)$$

H_{ev} is the interaction between metal electrons and the vibration of frequency ω_v of the adsorbate. 0 and 1 in the matrix element $\langle 1, i | H_{ev} | 0, i \rangle$ denote the number of vibrational quanta ω_v in the adsorbate. Because of the relaxation of the momentum conservation by the presence of the adatom, to which the adsorbate is bound, the interaction is much stronger than for an adsorbate bound to a smooth part of the surface. One should note that the relaxation of the momentum conservation rule for the H_{ep} matrix elements in formula (8) is caused by the adatom to which the adsorbate is bound. The arguments about the influence of the relaxation of the momentum conservation on H_{ep} with respect to formula (7) also apply to formula (8).

In the case of silver cyanide complexes, an experimental evidence for the strength of H_{ev} is given by the tenfold increase in infrared absorbance by the CN⁻ stretch vibration when CN⁻ is bound to Ag⁺ in solution [38]. Jones [47] explained this by dynamic charge transfer from the CN⁻ group to Ag⁺. In the case of silver cyanide surface complexes, one might expect a dynamic charge transfer from CN⁻ via Ag⁺ to the Ag metal. (This corresponds to mechanism b for H_{ev} in ref. [13]).

The proposed mechanism is not necessarily in contradiction to the experimentally observed frequency variation of the Raman cross section of pyridine adsorbed to silver, and the corresponding variation of the electro-reflectance coefficient with the frequency of the laser light measured by Pettinger, Wenning and Kolb [25]. (See also ref. [62].) As already pointed out in ref. [17], the atomic scale surface roughness will also induce additional absorption in the visible spectral range.

In our simple model, these roughness induced absorption processes are proportional to $|\langle e | H_{ep} | 0 \rangle|^2$ where e denote electron hole pairs with excitation energy $\hbar\omega_1$. The matrix element $\langle e | H_{ep} | 0 \rangle$ is similar to the matrix elements $\langle i | H_{ep} | 0 \rangle$ and $\langle k | H_{ep} | k, j \rangle^*$ in formulae (7) and (8) in the case of resonance because then the

electron hole pairs i and j have about the excitation energy $\hbar\omega_1$. Or, in different words: When the H_{ev} matrix element in (8) does not vary much with ω_i and ω_j , $\sigma(\omega_v)$ and $\sigma(\omega_k)$ will show the same dependence on ω_L . As explained in section 8, $\sigma(\omega_k)$ is approximately proportional to the fourth power of the roughness and adsorbate induced surface susceptibility.

The variation of the matrix elements with $\hbar\omega_1$ will depend on the variation with ω_L of the form factors mentioned in section 8. This effect can be incorporated in our simple model when $\langle i|H_{ep}|0\rangle$ is evaluated for the particular adsorbate–adatom–metal complex.

10. Comments

After having presented a possible explanation for the enhancement in sections 8 and 9, a discussion of some other hypothesis seems necessary and in order [63].

10.1. Resonant Raman effect by coupling to surface plasmons [10–12]

Raman scattering experiments on pyridine adsorbed on silver and gold sol particles have been performed by Creighton, Blatchford and Albrecht [5]. According to these authors, their experiments confirm, that surface plasma oscillations are involved in the intense Raman scattering. The main argument was the following: The sol particles showed an absorption spectrum with two maxima. According to Mie's scattering theory each maximum corresponds to a special particle diameter. The Raman cross section, taken as function of the exciting laser frequency matches qualitatively the cross section for elastic light scattering for the particles with greater diameter, as calculated from Mie's theory.

However, Creighton et al. give no explanation, why the analogous signal for the particles of smaller size was not observed at all. These experimental observations may also be explained in the following way: The excitation spectrum of the Raman cross section is the product of the macroscopic electrodynamic Mie scattering cross section and the excitation spectrum of the microscopically enhanced Raman cross section, as observed for pyridine on relatively smooth plane silver surfaces by Creighton et al. [62] and by Pettinger et al. [25]. The latter spectrum shows approximately a twentyfold stronger cross section at 600 nm than at 450 nm. (This cannot be explained by surface roughness coupling of light to surface plasmons, because this effect would be strongest near 360 nm.) Therefore, one would not expect a significant contribution from the silver sol particles of smaller size, because of the lower Mie scattering cross section and the low microscopic enhancement.

We consider a strong coupling of surface plasmons to adsorbates as very unlikely [64], because surface plasmon polaritons on a silver surface are delocalized on the scale of the adsorbate dimensions – they extend into the vacuum (or the liquid electrolyte) several thousand Å, and into the metal about 200–300 Å [65]. Only at

the limiting frequency ω_{sp} (corresponding for silver to 360 nm) the surface plasmons are fairly localized. Hence, only for adsorbates with an electronic excitation near ω_{sp} would one expect strong coupling between adsorbate and surface plasmons [66].

10.2. Image dipole effects.

King, Van Duyne and Schatz [9] have proposed a model, in which the dynamical dipolar moment of the adsorbate, induced by the laser beam is enhanced by the presence of the image dipole. The enhancement factor F is given by

$$F = \frac{3}{4} [1 + \gamma(\omega_L)^2] \left| 1 - \frac{\gamma(\omega_L) \alpha_e(\omega_L)}{4R^3} \right|^{-4},$$

$$\gamma(\omega_L) = \frac{\epsilon_m(\omega_L) - \epsilon_l(\omega_L)}{\epsilon_m(\omega_L) + \epsilon_l(\omega_L)}. \quad (9)$$

In (9), $\alpha_e(\omega_L)$ is the electronic polarizability of the adsorbate, $\epsilon_m(\omega_L)$ and $\epsilon_l(\omega_L)$ are the dielectric functions of the metal and the liquid electrolyte, all taken at the laser frequency ω_L . R is the distance adsorbate to metal surface. For small R , F can reach values of 10^5 to 10^6 .

Within the same model, the softening of the vibrational frequency ω_0 of the free adsorbate by the influence of the image dipole has been calculated by Lucas and Mahan [67]:

$$\omega = \omega_0 \{1 - \gamma(\omega) \alpha_v(0) / [4R^3 - \alpha_e(\omega)]\}^{1/2}. \quad (10)$$

Because $\gamma(\omega) \approx \gamma(\omega_L)$ and $\alpha_e(\omega) \approx \alpha_e(\omega_L)$, F and the vibrational softening

$$S = (\omega_0 - \omega) / \omega_0$$

are correlated.

For typical values $\alpha_e \sim 2 \text{ \AA}^3$ and $\alpha_v(0) \sim 0.05 \text{ \AA}^3$, one obtains $S = 0.2$ for $F = 10^5$ and $S = 0.8$ for $F = 10^6$. Near the maximum value of F , the molecule dissociated. However, Jeanmaire and Duyne [2] observed for pyridine on silver $S < 10^{-2}$ [54], but $F > 10^5$, which is not easily reconciled with the image dipole model [9,67]. Also the Raman experiments by Allen and Van Duyne on different cyanopyridines [68] do not show the strong dependence of the CN stretch signal on the distance R of the cyanide group from the metal surface according to formula (9), provided that the adsorption geometries as proposed in ref. [68] are correct.

The image dipole theory of King, Van Duyne and Schatz [9] is a good approximation to Efrima and Metiu's classic theory of light scattering by a molecule located near a solid surface [69]. In this sense, the arguments given above also hold for this theory.

11. Conclusion

The results of this paper may be summarized as follows:

- (1) A strong Raman enhancement for an adsorbate on a silver surface is only possible when the adsorbate is bound to an atomic scale surface roughness, e.g. an adatom.
- (2) The relaxation of the momentum conservation rule for scattering of metal electrons from an atomic scale surface roughness causes resonance Raman scattering at metal electrons and adsorbate vibrations.

This mechanism is a local one which is definitely different from models involving surface roughness induced surface plasmons [10–12].

The strength of the resonance effect will depend on the electron adatom scattering form factors. We conjecture that the proposed roughness induced enhancement mechanism should also exist for other metals besides Ag, Au, Cu, and Pt, for instance on Al. An adsorbate on a smooth surface is also a “roughness on atomic scale”. In general, the form factor for electron scattering from the adsorbate will be weaker than from an adatom, and therefore, the Raman cross section will not be increased so much. This is confirmed for atmospheric contaminants and cyanide on silver [6]: An evaporated smooth silver film exposed to air and cyanide solution will be covered at least with one monolayer of adsorbates, but no Raman signal could be detected (see also section 7).

Nevertheless, we do not exclude the possibility that the mechanisms mentioned in the introduction and in ref. [59] may cause some enhancement of the Raman cross section of adsorbates on smooth surfaces in special cases. Even so, we think that the resonance effect, introduced by the atomic roughness of the metal surface, is the most important enhancement mechanism.

Acknowledgements

We would like to thank W. Pütz and J. Heitbaum for performing the radiochemical measurement; F.E. Aussenegg, J.G. Bergman, E. Burstein, J. Heitbaum, P.J. Hendra, R.M. Hexter, D.M. Kolb, A. Lucas, B. Pettinger, W. Richter, W. Schaich, J.W. Schultze and R. Van Duyne for discussions and J.G. Bergman, E. Burstein, J.A. Creighton, T.E. Furtak, M.V. Klein, S.L. McCall and M. Moskovits for sending us their results prior to publication.

Note added in proof

Bruce Laube (United Technologies Research Center, East Hartford, Connecticut 06108, USA) has presented experimental data to us, indicating that the structures in the voltammograms (fig. 2), which we have assigned to Ag_2O , are probably due

to AgCN. In this case, in eqs. (2) and (3), n is greater than 1; eq. (4) should be replaced by $\text{Ag}(\text{metal}) + \text{CN}^- \rightarrow \text{AgCN}(\text{solid film}) + e$; and eq. (5) should be replaced by $\text{AgCN}(\text{solid film}) + (n - 1) \text{CN}^- \rightarrow \text{Ag}(\text{CN})_n^{(n-1)}(\text{aqueous})$. As the important point of our reasoning is the observation of the Raman signal after the reduction of a surface film (be it Ag_2O or AgCN), our conclusions do not depend on this particular point.

References

- [1] M. Fleischmann, P.U. Hendra and A.J. McQuillan, *Chem. Phys. Letters* 26 (1974) 163.
- [2] D.L. Jeanmaire and R.P. Van Duyne, *J. Electroanal. Chem.* 84 (1977) 1.
- [3] M.G. Albrecht and J.A. Creighton, *J. Am. Chem. Soc.* 99 (1977) 5215.
- [4] B. Pettinger and U. Wenning, *Chem. Phys. Letters* 56 (1978) 253.
- [5] J.A. Creighton, C.G. Blatchford and M.G. Albrecht, *J. Chem. Soc. Faraday II*, 75 (1979) 790.
- [6] A. Otto, *Surface Sci.* 75 (1978) L392.
- [7] T.H. Wood and M.V. Klein, *J. Vacuum Sci. Technol.* 16 (1979) 459.
- [8] R. Van Duyne, *J. Physique (Paris) Suppl.* C5 (1977) 239.
- [9] F.W. King, R. Van Duyne and G.C. Schatz, *J. Chem. Phys.* 69 (1978) 4472. S. Efrima and H. Metiu, *Chem. Phys. Letters* 60 (1978) 59.
- [10] M.R. Philpott, *J. Chem. Phys.* 62 (1975) 1812.
- [11] R.M. Hexter and M.G. Albrecht, *Spectrochim. Acta* 35A (1979) 233.
- [12] M. Moskovits, *J. Chem. Phys.* 69 (1978) 4159.
- [13] E. Burstein, Y.J. Chen and S. Lundquist, *Bull. Am. Phys. Soc.* 23 (1978) 30; E. Burstein, Y.J. Chen, C.Y. Chen, S. Lundquist and E. Tossatti, *Solid State Commun.* 29 (1979) 567.
- [14] J.I. Gersten, R.L. Birke and J.R. Lombardi, *Phys. Rev. Letters* 43 (1979) 147.
- [15] T.E. Furtak, *Solid State Commun.* 28 (1979) 903.
- [16] R. Fuchs, *Bull. Am. Phys. Soc.* 24 (1979) 339.
- [17] A. Otto, in: *Proc. Intern. Conf. on Vibrations in Adsorbed Layers*, Jülich, 1978, reprint available upon request.
- [18] S.L. McCall and P.M. Platzman, *Bull. Am. Phys. Soc.* 24 (1979) 340, and preprint.
- [19] C.Y. Chen and E. Burstein, *Bull. Am. Phys. Soc.* 24 (1979) 341.
- [20] F.R. Aussenegg and M.E. Lippitsch, *Chem. Phys. Letters* 59 (1978) 214.
- [21] T.E. Furtak, *Solid State Commun.* 23 (1977) 373.
- [22] B. Pettinger, private communication.
- [23] P.J. Hendra and M. Fleischmann, in: *Topics in Surface Chemistry*, Eds. E. Kay and P.S. Bagus (Plenum, New York, 1978) and references therein.
- [24] G. Hagen, B. Simic Glavaski and E. Yeager, *J. Electroanal. Chem.* 88 (1978) 269.
- [25] B. Pettinger, U. Wenning and D.M. Kolb, *Ber. Bunsenges. Physik. Chem.* 82 (1978) 1326.
- [26] G. Albrecht, J.F. Evans and J.A. Creighton, *Surface Sci.* 75 (1978) L777.
- [27] M. Pourbaix, *Atlas d'Equilibres Electrochimiques* (Gauthier-Villars, Paris, 1963).
- [28] A.J. Bard, *Encyclopedia of Electrochemistry of the Elements*, Vol. VII (Dekker, New York, 1976).
- [29] M. Moskovits and K.H. Michaelian, *J. Chem. Phys.* 69 (1978) 2306.
- [30] T.C. Waddington, *J. Chem. Soc.* (1959) 2499.
- [31] D. Britton and J.D. Dunitz, *Acta Cryst.* 18 (1965) 424.
- [32] W. Vielstich and H. Gerischer, *Z. Physik. Chem.* 4 (1955) 10.
- [33] E. Budewski, W. Bostanoff, T. Vitanoff, Z. Stoinoff, A. Kotzewa and R. Kaischew, *Phys. Status Solidi* 13 (1966) 577.

- [34] V. Bostanov, G. Staikov and D.K. Roe, *J. Electrochem. Soc.* 122 (1975) 1301.
- [35] J. Schmit and A.A. Lucas, *Solid State Commun.* 11 (1972) 419;
J. Friedel, *Ann. Physique (Paris)* 6 (1976) 262.
- [36] J.P. Young, *Plating* 54 (1967) 272.
- [37] H. Bassett and A.S. Corbet, *J. Chem. Soc.* 125 (1924) 1660.
- [38] L.H. Jones and R.A. Penneman, *J. Chem. Phys.* 22 (1954) 965.
- [39] R.M. Izatt, H.D. Johnston, G.W. Watt and J.J. Christensen, *Inorg. Chem.* 6 (1967) 132.
- [40] L.H. Jones, *J. Chem. Phys.* 26 (1957) 1578.
- [41] J.L. Hoard, *Z. Krist.* 84 (1933) 231, confirmed in ref. [42], see also ref. [40].
- [42] A. Rosenzweig and D.T. Cromer, *Acta Cryst.* 12 (1959) 709.
- [43] R.B. Roof, Jr., A.C. Larson and D.T. Cromer, *Acta Cryst. B*24 (1968) 269.
- [44] L.H. Jones, *Spectrochim. Acta* 19 (1963) 1675.
- [45] R. Gauffrès, *Compt. Rend. (Paris)* 252 (1961) 3227.
- [46] G.W. Chantry and R.A. Plane, *J. Chem. Phys.* 33 (1960) 736.
- [47] L.H. Jones, *Inorg. Chem.* 2 (1963) 777.
- [48] R.L. DeKock, A.C. Sarapu and R.F. Fenske, *Inorg. Chem.* 10 (1971) 38.
- [49] C.D. West, *Z. Krist.* 90 (1935) 555.
- [50] K.M. Griffing and J. Simons, *J. Chem. Phys.* 64 (1976) 3610.
- [51] W. Pütz and J. Heitbaum, *Inst. Physikalische Chemie, Univ. Bonn*, unpublished result.
- [52] J.G. Bergman, J.P. Heritage, A. Pinzcuk, J.M. Worlock and J.H. McFee, *Chem. Phys. Letters*.
- [53] K. Schwabe, K. Wagner and Ch. Weissmantel, *Z. Physik. Chem. (Leipzig)* 206 (1957) 309;
F. Cabanè-Brouty and J. Oudar, *Compt. Rend. (Paris)* 254 (1962) 471.
- [54] A small change in vibrational frequencies is consistent with Raman enhancement: for pyridine on silver, the breathing modes are changed only by 3 cm^{-1} by adsorption [2].
- [55] A cluster calculation for CO on Ni [56] may provide further evidence: second layer Ni atoms have little influence on the CO stretch frequency.
- [56] P. Politzer and S.D. Kasten, *J. Phys. Chem.* 80 (1976) 385.
- [57] L.H. Jones, *J. Chem. Phys.* 29 (1958) 463.
- [58] C.Y. Chen, E. Burstein and S. Lundquist, *Solid State Commun.* 32 (1979) 63; E. Burstein, C.Y. Chen and S. Lundquist, in: *Proc. US-USSR Symp. on The Theory of Light Scattering in Condensed Matter*, New York, 1979 (Plenum)
- [59] M.S.P. Lucas, *Appl. Phys. Letters* 4 (1964) 73.
- [60] R.M. Martin and L.M. Falicov, in: *Light Scattering in Solids*, Ed. M. Cardona (Springer, 1975).
- [61] A. Otto, J. Timper, J. Billmann, G. Kovacs and I. Pockrand, *Surface Sci.* 92 (1980) L55.
- [62] J.A. Creighton, M.G. Albrecht, R.E. Hester and J.A.D. Matthew, *Chem. Phys. Letters* 55 (1978) 55.
- [63] We have included this section, following the suggestion of one referee.
- [64] A. Otto, in: *Proc. Intern. Conf. on Non-Traditional Approaches to the Study of the Solid-Electrolyte Interface*, 1979, to be published.
- [65] A. Otto, in: *Advances in Solid State Physics*, Vol. XIV, Eds. O. Madelung and H.J. Queisser (Pergamon, 1974);
A. Otto, in: *Optical Properties of Solids, New Developments*, Ed. B.O. Seraphin (North-Holland, Amsterdam, 1976).
- [66] H. Morawitz, in: *Proc. NATO Summer School, 7th Course Intern. School of Quantum Electronics* (1977).
- [67] A.A. Lucas and G.D. Mahan, *Theory of Vibrations in Adsorbed Layers*, preprint.
- [68] C.S. Allen and R.P. Van Duyne, *Chem. Phys. Letters* 63 (1979) 455.
- [69] S. Efrima and H. Metiu, *J. Chem. Phys.* 70 (1979) 1602, 1939, 2297.